



HAL
open science

Analyzing the impact of pulsatile flow on drug release from a single strut of a drug-eluting stent

N. Abbasnezhad, M. Shirinbayan, S. Champmartin, F. Bakir

► To cite this version:

N. Abbasnezhad, M. Shirinbayan, S. Champmartin, F. Bakir. Analyzing the impact of pulsatile flow on drug release from a single strut of a drug-eluting stent. *Journal of Biomechanics*, 2023, 146, 10.1016/j.jbiomech.2022.111425 . hal-04072823

HAL Id: hal-04072823

<https://cnam.hal.science/hal-04072823v1>

Submitted on 8 Jan 2025

HAL is a multi-disciplinary open access archive for the deposit and dissemination of scientific research documents, whether they are published or not. The documents may come from teaching and research institutions in France or abroad, or from public or private research centers.

L'archive ouverte pluridisciplinaire **HAL**, est destinée au dépôt et à la diffusion de documents scientifiques de niveau recherche, publiés ou non, émanant des établissements d'enseignement et de recherche français ou étrangers, des laboratoires publics ou privés.

Copyright

Analyzing the impact of pulsatile flow on drug release from a single strut of a drug-eluting stent

N. Abbasnezhad^{1,2*}, M. Shirinbayan^{1,2}, S. Champmartin¹, F. Bakir¹

¹Arts et Metiers Institute of Technology, CNAM, LIFSE, HESAM University, F-75013 Paris, France, mohammadali.shirinbayan@ensam.eu, stephane.champmartin@ensam.eu, farid.bakir@ensam.eu

²Arts et Metiers Institute of Technology, CNAM, PIMM, HESAM University, F-75013 Paris, France

*Correspondence: navideh.abbasnezhad@ensam.eu

Abstract: In this study, in-vitro experiments were performed to investigate the drug release from a single strut of a drug-eluting stent with respect to the systolic-diastolic flow and the continuous flow. Regarding, a test bench comprising a single strut and agarose gel as an arterial wall model was designed. The model chosen represents a large-scaled strut of a stent, to limit the effect of the geometrical shape of the stents on the drug release results. The comparison is carried out between two continuous flow rates and a systolic-diastolic flow pattern varying between these two flow rates, with a frequency of 70 beats per minute. The stent model is a polylactic-co-glycolic acid film (50:50) loaded with 10% diclofenac sodium. A compartment of agarose gel (1%) and a phosphate-buffered saline solution at 37°C are employed to mimic the arterial wall and the blood, respectively. Our results show the importance of flow type on the drug release from the stent and distribution of drug in the hydrogel, such that the pulsatility promotes an increase in the quantity of drug absorbed into the hydrogel.

Keywords: Systolic-diastolic flow, Continuous flow, Drug release, Agarose hydrogel

1. Introduction

Cardiovascular diseases (CVD) are the leading cause of death in developed countries including hypertension, coronary heart disease (CHD), stroke, and lower extremity arterial disease (LEAD) (Bink et al. 2019; Hu et al. 2018). The most common cause of CVD is atherosclerosis which is caused by a local aggregation of blood and blood products, complex carbohydrates, lipids, and calcium deposits in large and medium-sized arteries, accompanied by modifications in the artery (Ferreira et al. 2018). The treatment applied over recent years is using drug-eluting stents (DESs), which are still in development. In this regard, many experimental tests have been done in vitro, ex vivo, or in vivo. Having trustworthy test results need a reliable test setup with consistent test conditions, which simulates the real condition (Stein et al. 2018). As an important example over the last few decades, hemodynamics for diseased arteries has been extensively investigated (Fan et al. 2021; Wong et al. 2020) and the effect of the continuous flow on the release of the drug is not hidden anymore (Bernad et al. 2021). In most in vitro studies, the continuous flow was performed for analyzing the release profile from drug-eluting stents. Some studies have shown experimentally or numerically the effect of the different flow rates on the drug release at the continuous state (Wang et al. 2021). Seidlitz et al. (Seidlitz et al. 2011) studied the effect of different flow rates, 35 and 4 ml/min, in continuous and stationary flow for two different types of drugs, fluorescein sodium and triamterene. They showed that the release and distribution of hydrophilic fluorescein sodium were prone to change with flow rate. On the other hand, triamterene release was not influenced by the flow rate. This dissimilar response of the two model compounds to the variation of the flow rate emphasizes the need for a case-by-case examination of different compositions of drug carriers.

To characterize the influence of the luminal flow on drug diffusion in the arterial wall, it is important to consider many aspects associated with blood flow. Systolic-diastolic blood flow pattern induced by the cardiac pulse produces a complex flow nature (Sood et al. 2018). The pulsatile nature of blood flow in arteries consists of a steady component and its oscillating harmonics consist of amplitude and frequency. It is a time-dependent behavior in which its pattern depends on geometry, Reynolds number, arterial

45 wall compliance, and non-Newtonian viscosity of the blood. However, the mechanisms that regulate the
46 drug release in the pulsatile flow remain an unanswered question.
47 Ku et al. (Ku and Giddens 1983) have compared the behavior of the continuous flow and pulsatile flow in
48 the bifurcation without considering drug transport. Their results showed that the pulsatile flow had a
49 different character of flow, especially at the bifurcations. Whereas the steady flow showed a fixed
50 separation of the flow, without any turbulence and wall shear stress which is rather constant during the
51 time. In a study by O'Brien et al. (O'Brien C, Kolachalama V 2013) the effect of pulsatile flow on drug
52 release is investigated. The results demonstrated considerable sensitivity to the spatial pattern of drug
53 distribution when pulsatile flow amplitude was changed, but less sensitive to the impact on drug
54 absorption. In the literature, numerical and experimental studies on the significant influence of the
55 Reynolds number on drug release have been conducted (Mandal and Mandal 2018; O'Brien C,
56 Kolachalama V 2013; Saha and Mandal 2018). Such that, two times reduction in the Reynolds number has
57 been accompanied by a 28.8% increase in the hydrogel's total drug uptake (O'Brien C, Kolachalama V
58 2013). Additionally, the numerical analysis showed an increase in the drug release in the lumen by
59 enhancing this number (Saha and Mandal 2018).

60 To our best knowledge, there is a lack of experimental studies on the effect of the pulsatile flow on
61 the drug release from a strut of a drug-eluting stent. This research investigates the effect of pulsatile and
62 continuous flow on drug release in the lumen and hydrogel. Two different steady-state flow rates related
63 to the systolic and diastolic values, and the pulsatile flow varying between these values are considered.

64 2. Materials and Methods

65 2.1. Materials

66 Polylactic-co-glycolic acid (PLGA), with a molar ratio of 50-50 (D,L-lactic to glycolic acid), M_w (molecular
67 weight) = 38000-54000 g/mol, was used as a drug carrier. Diclofenac Sodium (DS), with water solubility of
68 2.37 mg/l at 25 °C and molecular weight of 318.13 g/mol, was used as an active substance model. Ethyl
69 acetate was used as the solvent of the PLGA. Phosphate buffered saline (PBS) and molecular biology
70 grade agarose were used as blood flow and the artificial tissue simulator, respectively. All the mentioned
71 components were purchased from Sigma Aldrich.

72 2.2. Sample preparation

73 For each set of films 20% w/v polymer to the solvent (ethyl acetate), was prepared with 10 wt.%
74 diclofenac sodium, which means for 1 g of PLGA, 0.1 g drug was added. The solution was agitated by a
75 magnetic stirrer at 600 rpm for about 1 hour at 40 °C. The method of casting in the Teflon-coated mold
76 (Abbasnezhad et al. 2020), was used for sample preparation. The procedure was followed by drying the
77 samples at room temperature for 24 hours. Finally, the mold was placed in the vacuum oven at the
78 temperature of 40 °C for 24 h. The samples were cut in rectangular form with dimensions of 0.3×5×30
79 mm³. This geometry was chosen to limit the effect of the geometrical shape of the stents on the drug
80 release results, representing a strut of a stent with a scale factor of 40.

81 2.3. Hydrogel preparation

82 Depending on the setup environmental conditions to analyze the drug released from the stents, some
83 properties of the hydrogels such as mechanical properties, degradation, and swelling are among the
84 selection factors. The choice of agarose in this study is motivated by its long-term stability, its mechanical
85 properties, and the close value of the diffusion coefficient to that of the arterial tissue (Semmling et al.
86 2013; Tzafiriri et al. 2012). The agarose hydrogel was prepared at 1% (w/w) concentration to simulate the
87 vessel wall, where for 0.1 g of agarose powder 10 ml PBS was used. The agarose was dissolved in water

88 heated to 100 °C and stirred on a magnetic stirrer until optically clear solutions were obtained. During
89 this period, the container was tightly closed to avoid evaporation and change in concentration. Later, the
90 temperature was lowered to 60 °C. After that, the samples were poured into the chambers considered for
91 the hydrogel, and then they were cooled until gelation.

92 2.3.1 Calculation of the diffusion coefficient of hydrogel

93 The permeability of the agarose gel is experimentally evaluated under the static flow condition. For this, a
94 volume of (4 ml) 1% weight/volume (w/v) agarose was prepared (the same procedure that was used for
95 the hydrogel preparation). Next, it was poured into a syringe of 12 ml capacity, which was cut at the
96 needle side (shown in Figure 1). After the gelation of the agarose in the syringe, the remaining volume of
97 the syringe is filled with a solution containing a precise dose of the drug (50 mg of DS per 1 ml PBS
98 solution). These syringes are withdrawn at three various times and each time the undiffused solution is
99 emptied. Next, the drug-soaked hydrogel is cut into slices of 4 mm thickness so that they are used to
100 quantify, by the UV-Vis technique, the amount of drugs that they contain.

101
102 Then the value of the diffusion coefficient was calculated by using the below equation. The value
103 obtained in this regard was about $1.12 \times 10^{-4} \text{ mm}^2/\text{s}$. $\frac{C(x,t)}{C_0} = \text{erfc}\left(\frac{x}{2\sqrt{Dt}}\right)$
104 Eq. 1

105 here $C(x, t)$ is the concentration of the drug diffused in the gel at distance of x at time t , C_0 is the initial
106 concentration of the drug in the solution.

107 2.4. Release test bench

108 For the drug release, a closed-loop test bench was designed. The components are depicted in Figure 2.
109 The samples were placed in the test chamber (1). The temperature of the fluid in the system was heated
110 with an electric resistance (2) to be always in the range of 37 ± 0.5 °C. To drive the impeller of the
111 centrifugal pump (3), a direct current motor, a Maxon EC-4-pole motor was used (4). It is connected to an
112 ESCON-Maxon servo controller (5). This controller is linked to a National Instruments acquisition card
113 (NI USB-6008) (6). This card, controlled by LabView, generates the commands of the pulsed wave
114 patterns and the number of pulses per minute conveyed to the servo controller. Figure 3 shows the
115 chosen waveform, which is of the carotid artery. Additionally, the acquisition card collects information
116 from the sensors. Flowmeters of FT-110 Series-TurboFlow (7), a pressure sensor (8) of the type JUMO
117 MIDAS SI, and a Class A PT100 resistive probe (9) for monitoring the temperature, as the sensors, in this
118 study were used. A reservoir (10) and a magnetic-drive pump (11), for containing and damping the fluid,
119 were implemented in the system. By-pass (12), valves (13) and distributors (14) were the additional
120 elements in the system to control the flow.

121 2.5. In vitro drug release procedure and associated measurement

122 UV-Vis spectrophotometry lambda 35 was used to determine the concentration of Diclofenac sodium
123 released in 1L of PBS solution and diffused into the agarose hydrogel after determined time points. The
124 hydrogel was placed in a compartment (with the dimensions of $130 \times 30 \times 1 \text{ mm}^3$) situated in the bottom
125 wall of the test chamber; then the polymeric samples were placed on the hydrogel (Figure 4). The
126 polymeric samples were fixed with small clips on the surface of the agarose hydrogel, in order not to
127 move with the flow.

128 At each time step, the polymeric sample was removed. Then the agarose hydrogel was collected from the
129 compartment for analysis, and it was replaced with the new one, prepared beforehand. Next, the
130 polymeric sample was carefully placed on the new hydrogel to continue the test. At the same time steps,

131 4 ml of the PBS solution was sampled from the reservoir for studying the drug release in the PBS
132 medium. The statistical analysis is related to the number of tests performed (n=3) that is expressed as
133 mean \pm standard deviation in the release curves. To calculate the cumulative drug release, the total
134 amount of DS loaded on the PLGA polymer was also measured after degrading completely the polymer
135 film in ultrasound at high temperature. To establish the calibration curve of measurements, known
136 concentrations of DS in PBS and agarose hydrogel (1%) were measured. The following calibration
137 equations were found with the correlation coefficient of $R^2 = 0.99$ (shown in Figure 5).

138 This comparison of the released results is performed for two steady-state flows at 7.5 and 15 ml/s
139 (corresponding respectively to the pressures of 75 and 112 mmHg), and the pulsed flow that varies
140 between these values (shown in Figure 3) at 70 heartbeats per minute. These values were chosen from the
141 literature representing the waveform of the blood flow in the carotid (Sood et al. 2018; Yao et al. 2015).

142 3. Results and discussion

143 3.1. *In vitro* drug release at the continuous steady and unsteady flow

144 Figure 6 (a), and (b) show the results of DS release from the PLGA samples into the PBS medium and the
145 hydrogel compartment. Comparing these two figures indicate that, in all cases, there is much more
146 quantity released in the PBS than in the hydrogel. It is in a 1 to 10 ratio. Figure 6 (a) shows that by
147 increasing the flow rate from 7.5 to 15 ml/s the drug release rate in the PBS is increased at certain time
148 points. For example, after 12 h of release, for the flow rate of 15 ml/s about 55% of the drug is released
149 whereas for 7.5 ml/s about 46% of the drug is released. However, this difference is not much notable at
150 the other time points. It is noteworthy that also in these cases the release curves are following the same
151 tendency. Besides comparing the drug release results, in the steady-state (flow rates: 7.5 and 15 ml/s) with
152 the pulsed flow, one can note a meaningful difference in the release rates. In the case of pulsed flow, the
153 release rate is much higher than in the steady flow, especially in the second period of the release after the
154 burst phenomenon. As an example, at 30 h of release in the steady state about 70% of the drug is released,
155 whereas in the pulsatile flow about 80% of the drug is released. Nevertheless, the results show that for all
156 the flow rates, approximately 90% of the drug is released into the PBS at the time of 192 h. Figure 6 (b)
157 shows the drug concentration penetrated the hydrogel in accordance with the release time. The
158 controlling mechanism of the drug transport into the hydrogel is diffusion (Khodadadi Yazdi et al. 2020).
159 At first, the existence of high drug concentration gradients explains the rapid growth of the curves. At
160 steady-state, for two different flow rates of 7.5 ml/s and 15 ml/s, the amount of the drug diffused into the
161 hydrogel is rather within the same range. In contrast, the results for the pulsed flow show that the
162 amount of drug diffused into the hydrogel is higher than in the steady cases. This variance is almost
163 notable in the time points between 30 and 60 h with a difference of 1-1.5% release.

164 To analyze these results more deeply, the microstructure of the samples has been observed under a
165 Scanning Electron Microscopy (SEM).

166 Figure 7 shows the SEM micrographs of the PLGA samples with 10% of DS (a) before, and after 48 hours
167 of release test at (b) the steady flow of 7.5 ml/s and (b) unsteady flow. The figures are captured from the
168 luminal side of the polymer layer. By comparing these figures, one can note in both situations (steady and
169 unsteady), the creation of pores and the wrinkling of the polymer during the release. Thus, it denotes the
170 presence of the swelling and diffusion mechanisms in both cases. Depending on the other environmental
171 conditions such as pressure or the contribution of other mechanisms such as erosion, the pores can blast
172 and make the polymer surface more porous and suitable for drug release. It is evident that diffusion is
173 affected by the swelling phenomenon; its rate increases by increasing the space between the polymer
174 chains and the free volume in the polymer. Contrarily, the enlargement of the polymeric samples due to

175 the swelling, increases the migration distance for the release of the drug (Scheler 2014). Another
176 mechanism contributing to the drug release from the PLGA polymeric films is the mechanism of
177 degradation/erosion which results in the cleavage of polymer chains and can help the drug release.

178 From the mechanistic standpoint, it is notable that by increasing the flow rate, the thickness of the
179 hydrodynamic and mass boundary layers is getting smaller (Kleinstreuer 2018). Figure 8 shows a
180 demonstration of this conception. Moreover, in a review article by Rana et al. (Rana and Neeves 2016), it
181 is mentioned that by increasing the velocity, a thin boundary layer near the bottom layer of an arterial
182 wall, is constructed which results in a great Peclet number and therefore results in higher convective flux
183 than diffusive flux. Also, this fact can lead to the weakening of the mechanical behavior of the polymer
184 and an increase in the rate of erosion (Abbasnezhad et al. 2021). Our experimental results are in
185 agreement with the numerical study by Chen et al. (Chen et al. 2015), concerning the steady case at the
186 flow rates of 7.5 and 15 ml/s. Regarding this, a high value of Re number in steady-state conditions causes
187 an enhanced drug release rate in polymer and a lower drug concentration in tissue.

188 The former discussion is consistent with the obtained results, which indicates that on the lumen side, by
189 increasing the flow rate, convective flux is larger near the sample surface. This causes higher
190 concentration gradients of the drug between the polymer sample and the fluid, leading to higher
191 diffusive flux. Consequently, for the steady-state cases, increasing the flow rate, increases the diffusion of
192 the drug through the polymer, resulting in more drug release from the polymeric samples. One can note
193 that the drug release from the polymeric films in the case of unsteady pulsed flow compared to the steady
194 case is also higher. This is an effect of the flow pulsatility on the enhancement of the drug transfer as
195 already noted in a study by Chabi et al. (Chabi 2017). It is noteworthy that the analysis of the boundary
196 layer in the case of pulsed flow is not as easy. However, it can be explained by other conceptions. For
197 example, in a study by Ku (Ku 1997) on the blood flow in the arteries, it is mentioned that pulsatility
198 creates a periodic generation of turbulence. It reaches the maximum during the deceleration of systole
199 and the minimum during the upstroke of systole, where time and frequency are the reasons for this
200 transition to turbulence. Moreover, it is shown in (Kleinstreuer 2018) that increasing the turbulence in the
201 flow, increases the convective flux. These observations confirm our mass transfer results, where, in the
202 unsteady case due to the creation of turbulence the mass transfer is higher compared to the steady case.
203 Furthermore, in another study by O'Brien et al. (O'Brien C, Kolachalama V 2013) they demonstrated that
204 the drug deposition in the recirculation zone is shown to be dependent on the pulsed flow at various
205 Womersley numbers. It was observed that decreasing the Womersley number results in longer
206 recirculation, confirming our experimental results by indicating that the drug concentration is impacted
207 by the flow recirculation zone. Therefore, the disturbance of the velocity profile in the pulsed case and the
208 generation of the potential more vorticity is believed to be the cause of the increased release rate in the
209 hydrogel and PBS.

210 **4. Study limitations:**

211 Some of the limitations of this study are as follows: the complication of considering the biological
212 reactions, response of the cells to the foreign substances, and the inflammatory reactions, which is
213 complicated to be considered in the in vitro case; considering the filtration aspect in closed-loop systems.
214 Moreover, malpositioning the DES can also have a significant impact on the outcomes of the release.

215 **5. Conclusions**

216 In this study, a system capable of simulating both lumen and arterial tissue was developed. In this
217 regard, the blood flow, continuous or pulsatile, is reproduced via a pumping system. The arterial
218 medium is mimicked using a specific agarose compartment. The results showed the impact of the flow

219 pulsatility, especially at some periods of diffusion in the hydrogel on the release kinetics. This expresses
220 the usefulness of considering the pulsatility for a realistic simulation of drug release.

221 Abbasnezhad, N., Shirinbayan, M., Tcharkhtchi, A., and Bakir, F. (2020). "In vitro study of drug release
222 from various loaded polyurethane samples and subjected to different non-pulsed flow rates."
223 *Journal of Drug Delivery Science and Technology*, Elsevier, 55(December 2019), 101500.

224 Abbasnezhad, N., Zirak, N., Shirinbayan, M., Tcharkhtchi, A., and Bakir, F. (2021). "On the importance of
225 physical and mechanical properties of PLGA films during drug release." *Journal of Drug Delivery
226 Science and Technology*, 102446.

227 Bernad, S. I., Craciunescu, I., Sandhu, G. S., Dragomir-Daescu, D., Tombacz, E., Vekas, L., and Turcu, R.
228 (2021). "Fluid targeted delivery of functionalized magneto-responsive nanocomposite particles to a
229 ferromagnetic stent." *Journal of Magnetism and Magnetic Materials*, 519, 167489.

230 Bink, N., Mohan, V. B., and Fakirov, S. (2019). "Recent advances in plastic stents: a comprehensive
231 review." *International Journal of Polymeric Materials and Polymeric Biomaterials*, Taylor & Francis, 0(0),
232 1–22.

233 Chabi, F. (2017). "Etude numérique et expérimentale du transfert de masse, par advection et diffusion en
234 écoulement pulsé, sur des stents actifs. Fatih Chabi To cite this version: HAL Id: tel-01512747."

235 Chen, Y., Xiong, Y., Jiang, W., Yan, F., Guo, M., Wang, Q., and Fan, Y. (2015). "Numerical simulation on
236 the effects of drug eluting stents at different Reynolds numbers on hemodynamic and drug
237 concentration distribution." *Biomedical engineering online*, 14 Suppl 1(Suppl 1), S16.

238 Fan, Z., Liu, X., Zhang, Y., Zhang, N., Ye, X., and Deng, X. (2021). "Hemodynamic Impact of Stenting on
239 Carotid Bifurcation: A Potential Role of the Stented Segment and External Carotid Artery."
240 *Computational and Mathematical Methods in Medicine*, (G. Pontrelli, ed.), Hindawi, 2021, 7604532.

241 Ferreira, J. A., Gonçalves, L., Naghipoor, J., de Oliveira, P., and Rabczuk, T. (2018). "The effect of plaque
242 eccentricity on blood hemodynamics and drug release in a stented artery." *Medical engineering &
243 physics*, England, 60, 47–60.

244 Hu, T., Yang, C., Lin, S., Yu, Q., and Wang, G. (2018). "Biodegradable stents for coronary artery disease
245 treatment: Recent advances and future perspectives." *Materials Science and Engineering C*, Elsevier,
246 91(April), 163–178.

247 Khodadadi Yazdi, M., Taghizadeh, A., Taghizadeh, M., Stadler, F. J., Farokhi, M., Mottaghtalab, F.,
248 Zarrintaj, P., Ramsey, J. D., Seidi, F., Saeb, M. R., and Mozafari, M. (2020). "Agarose-based
249 biomaterials for advanced drug delivery." *Journal of controlled release: official journal of the Controlled
250 Release Society*, Netherlands, 326, 523–543.

251 Kleinstreuer, C. (2018). *Modern fluid dynamics*. Springer.

252 Ku, D. N. (1997). "Blood flow in arteries." *Annual Review of Fluid Mechanics*, 29, 399–434.

253 Ku, D. N., and Giddens, D. P. (1983). "Pulsatile flow in a model carotid bifurcation." *Arteriosclerosis*, 3(1),
254 31–39.

- 255 Mandal, A. P., and Mandal, P. K. (2018). "Distribution and retention of drug through an idealised
256 atherosclerotic plaque eluted from a half-embedded stent." *International Journal of Dynamics and*
257 *Control*, Springer Berlin Heidelberg, 6(3), 1183–1193.
- 258 O'Brien C, Kolachalama V, B. T. (2013). "Impact of flow pulsatility on arterial drug distribution in stent-
259 based therapy." *J Control Release*, 23(1), 1–7.
- 260 Rana, K., and Neeves, K. B. (2016). "Blood flow and mass transfer regulation of coagulation." *Blood*
261 *Reviews*, Elsevier Ltd, 30(5), 357–368.
- 262 Saha, R., and Mandal, P. K. (2018). "Effect of flow pulsatility and time-dependent release kinetics on
263 stent-based delivery through atherosclerotic plaque." *International Journal of Dynamics and Control*,
264 Springer Berlin Heidelberg, 6(1).
- 265 Scheler, S. (2014). "The polymer free volume as a controlling factor for drug release from poly(lactide-co-
266 glycolide) microspheres." *Journal of Applied Polymer Science*, 131(1), 1–13.
- 267 Seidlitz, A., Nagel, S., Semmling, B., Grabow, N., Sternberg, K., and Weitschies, W. (2011). "Biorelevant
268 dissolution testing of drug-eluting stents: Experiences with a modified flow-through cell setup."
269 *Dissolution Technologies*, 18(4), 26–35.
- 270 Semmling, B., Nagel, S., Sternberg, K., Weitschies, W., and Seidlitz, A. (2013). "Development of
271 Hydrophobized Alginate Hydrogels for the Vessel-Simulating Flow-Through Cell and Their Usage
272 for Biorelevant Drug-Eluting Stent Testing." *AAPS PharmSciTech*, 14(3), 1209–1218.
- 273 Sood, T., Roy, S., and Pathak, M. (2018). "Effect of pulse rate variation on blood flow through
274 axisymmetric and asymmetric stenotic artery models." *Mathematical Biosciences*, Elsevier Inc., 298, 1–
275 18.
- 276 Stein, S., Auel, T., Kempin, W., Bogdahn, M., Weitschies, W., and Seidlitz, A. (2018). "Influence of the test
277 method on in vitro drug release from intravitreal model implants containing dexamethasone or
278 fluorescein sodium in poly (D,L-lactide-co-glycolide) or polycaprolactone." *European Journal of*
279 *Pharmaceutics and Biopharmaceutics*, Elsevier, 127(November 2017), 270–278.
- 280 Tzafiriri, A. R., Groothuis, A., Price, G. S., and Edelman, E. R. (2012). "Stent elution rate determines drug
281 deposition and receptor-mediated effects." *Journal of Controlled Release*, Elsevier B.V., 161(3), 918–926.
- 282 Wang, J., Kural, M. H., Wu, J., Leiby, K. L., Mishra, V., Lysyy, T., Li, G., Luo, J., Greaney, A., Tellides, G.,
283 Qyang, Y., Huang, N., and Niklason, L. E. (2021). "An ex vivo physiologic and hyperplastic vessel
284 culture model to study intra-arterial stent therapies." *Biomaterials*, 275, 120911.
- 285 Wong, K. K. L., Wu, J., Liu, G., Huang, W., and Ghista, D. N. (2020). "Coronary arteries hemodynamics:
286 effect of arterial geometry on hemodynamic parameters causing atherosclerosis." *Medical &*
287 *Biological Engineering & Computing*, 58(8), 1831–1843.
- 288 Yao, Y., Hao, L., Geng, N., Jin, Y., Du, S., and Xu, L. (2015). "Estimation of carotid artery pressure
289 waveform by transfer function and radial pressure waveform." *Proceedings of the World Congress on*
290 *Intelligent Control and Automation (WCICA)*, 2015-March(March), 6090–6093.

List of figures

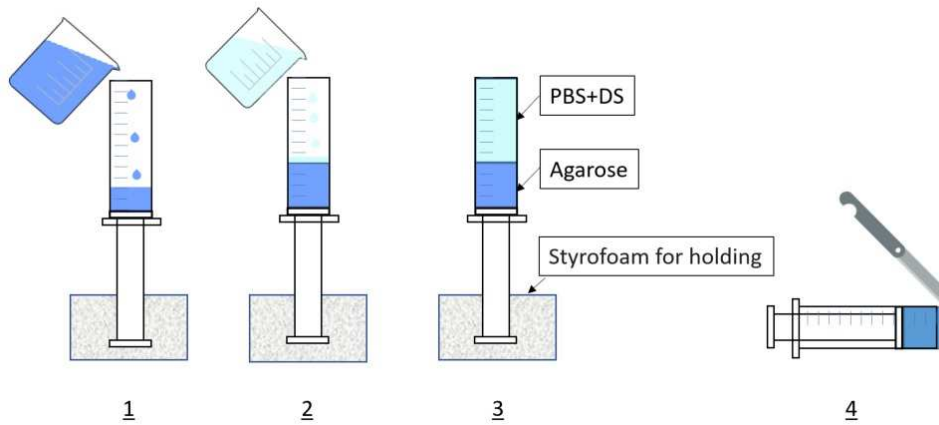


Figure 1. Procedure to measure the diffusion coefficient of the drug in gel

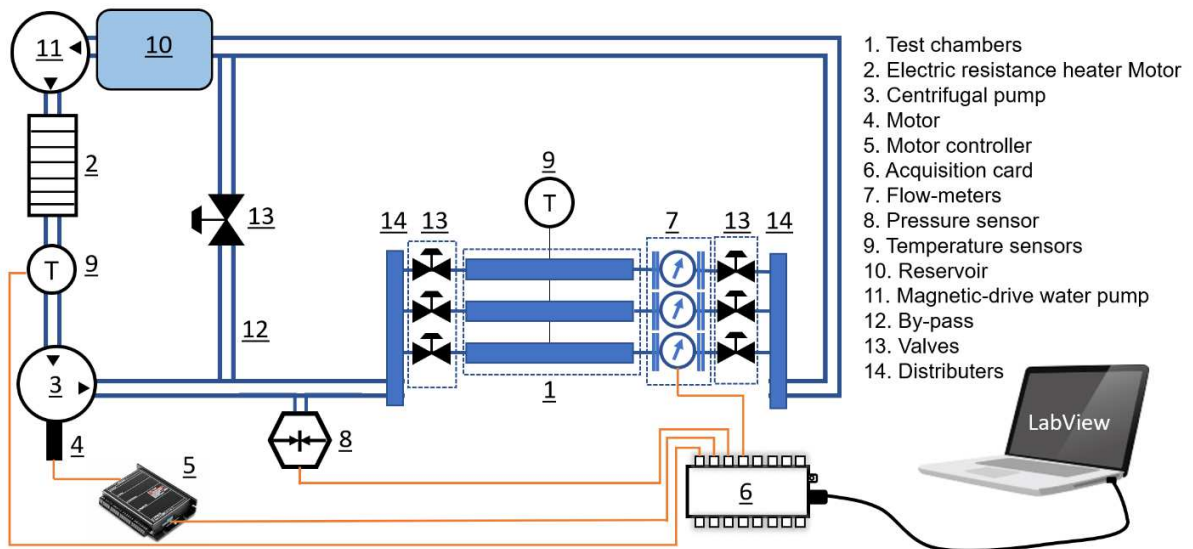


Figure 2. Schematic of the test bench

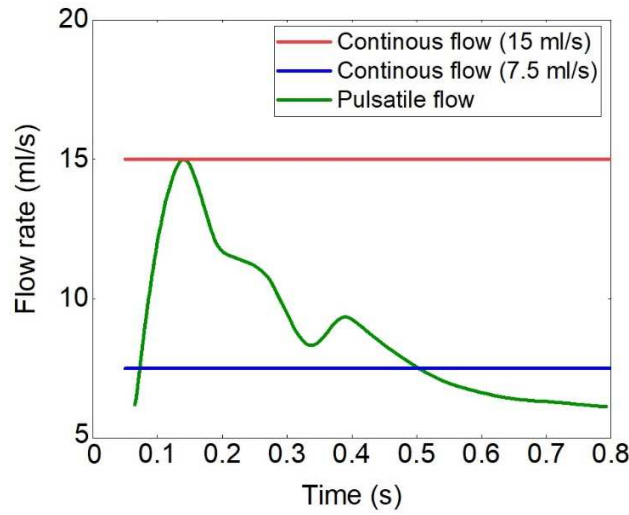


Figure 3. Flow rates related to the three patterns of the flow performed in this study

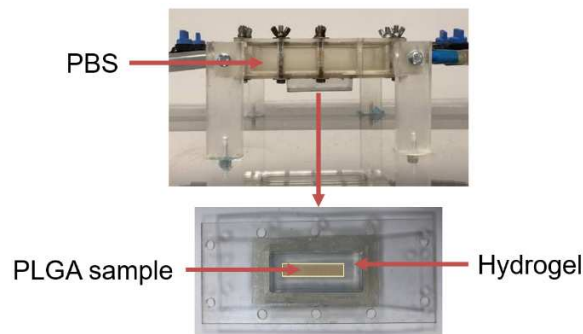


Figure 4. The compartment containing the hydrogel and the polymeric samples

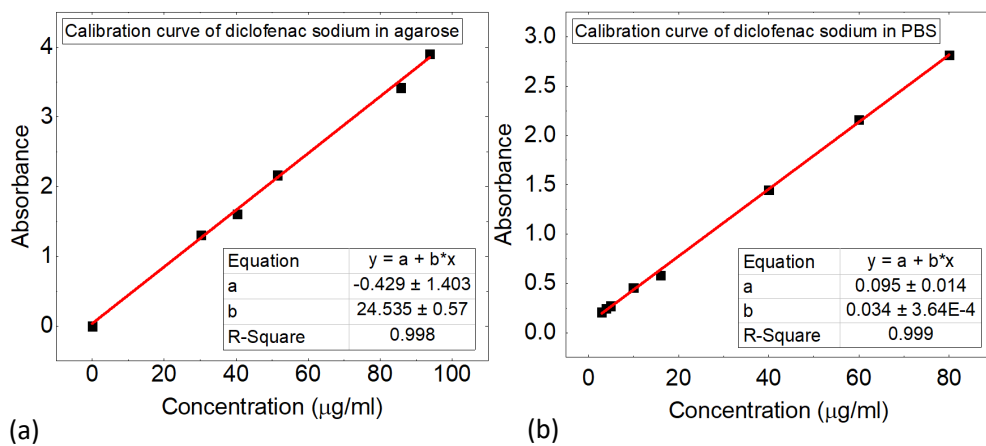


Figure 5. Calibration curves obtained for the diclofenac sodium in (a) hydrogel agarose and (b) PBS

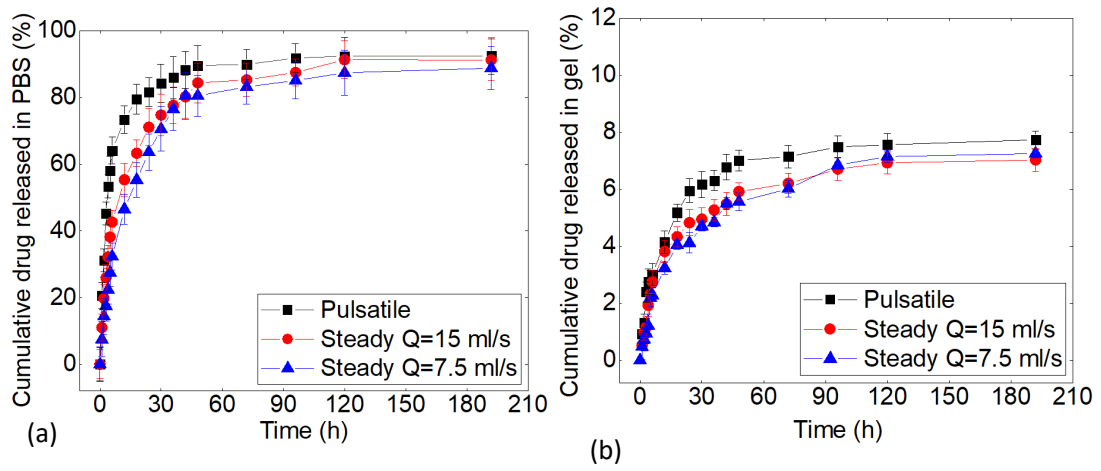
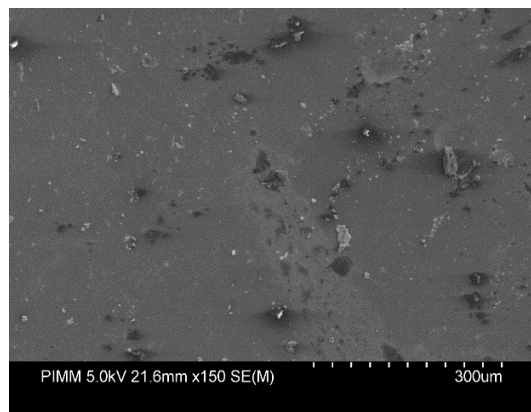
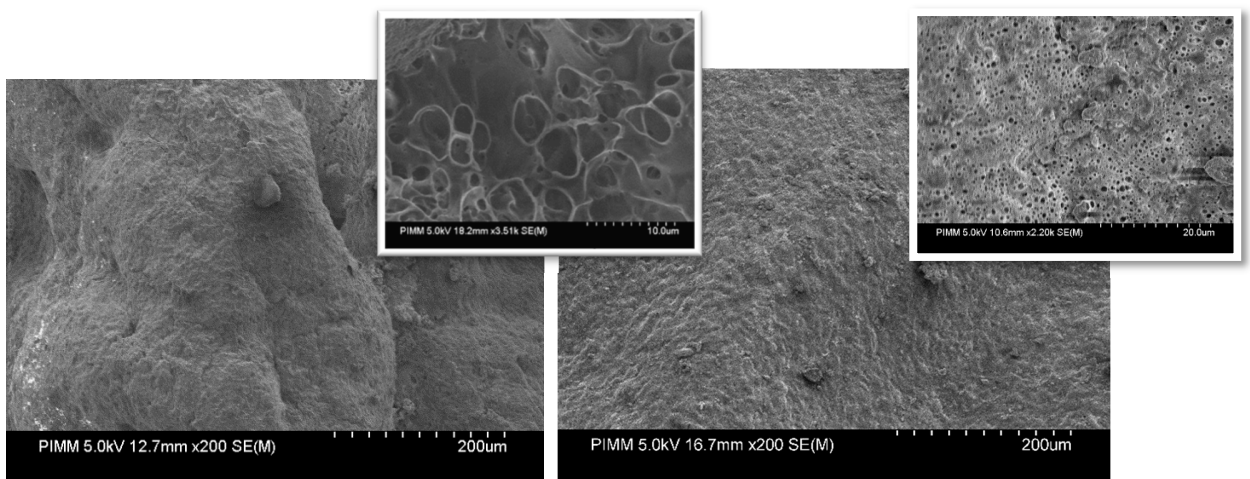


Figure 6. Drug release from the PLGA films with 10% DS at different flow rates in (a) PBS and (b) hydrogel



(a)



(b)

(c)

Figure 7. SEM micrographs of PLGA-10%DS samples from the side, contacted with the fluid at (a) $t=0$; and after 48h at the (b) steady flow with the flow rate of 7.5 ml/s and (b) pulsatile flow, at different magnifications

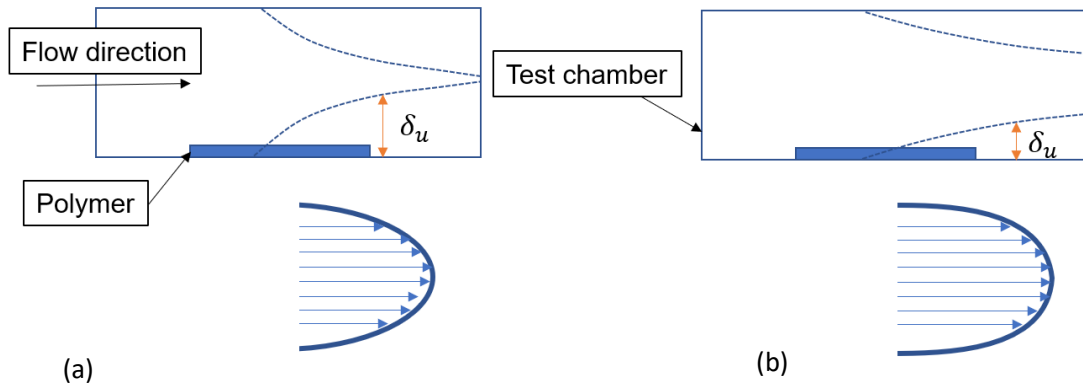


Figure 8. Schematic representing the thickness of boundary layers created at two different flow rates, (a) is for the case with a higher flow rate than (b), δ_u represents the thickness of the mass boundary layer